

⁹A rough analysis of the magnetoresistivity curves of AuFe alloys (Ref. 6), using the formulas of Ref. 1, indicates that for AuFe, $V > |J|$, and the orders of magnitude are $J \approx -0.75$ eV, $V \approx 3$ eV. In addition, susceptibility measurements indicate the spin S to be $3/2$; see O. S. Lutes and J. S. Schmit, Phys. Rev. **134**, A676 (1964); E. Scheil, H. Specht, and E. Wachtel, Z. Metallk. **49**, 590 (1958); B. Dreyfus, J. Souletie, J. L. Tholence, and R. Tournier, Appl. Phys. **39**, 846 (1968); C. M. Hurd, Phys. Chem. Solids **28**, 1345 (1967).

¹⁰The fact that a formally higher-order term is larger numerically is a consequence of the slow convergence of the logarithmic series for the scattering amplitudes, which has been noted before (Ref. 1). As we have mentioned in that reference, this implies that perturbative

calculations such as this one can reproduce the qualitative features of the experimental behavior, e.g., low-field dependence on M^2 , but estimates of J and V from explicit use of these perturbative formulas are valid only for the relative orders of magnitude.

¹¹A. M. Guénault (private communication quoted in Ref. 5).

¹²D. K. C. Macdonald, W. B. Pearson, and I. M. Templeton, Proc. Roy. Soc. (London) **A266**, 161 (1962).

¹³Incremental susceptibility measurements on CuCr [M. D. Daybell, W. P. Pratt, Jr., and W. A. Steyert, Phys. Rev. Letters **22**, 401 (1969)] indicate that for $T \ll T_K$, T_K the Kondo temperature, the impurity magnetization does not saturate for $g\mu_B H/kT \gg 1$, but for $g\mu_B H/kT_K \gg 1$.

Polarization Fluctuations and the Optical-Absorption Edge in BaTiO₃[†]

S. H. Wemple

Bell Telephone Laboratories, Murray Hill, New Jersey 07974

(Received 13 March 1970)

Results of optical absorption and electroabsorption (EA) measurements in the vicinity of the interband absorption edge are reported for top-seeded solution-grown crystals of BaTiO₃. In common with other perovskite oxides, the absorption edge in BaTiO₃ is found to display Urbach-rule behavior. The exponential absorption tail can be described between 20 and 450 °C by an effective temperature $T^* = T + T_0$, where $T_0 = 140$ °K, i.e., $\alpha \propto e^{\hbar\omega/kT^*}$. Although no uniquely defined band gap can be extracted from an exponential edge, we propose, on the basis of indirect arguments, that the room-temperature band gaps are 3.38 and 3.27 eV, respectively, for light polarized parallel and perpendicular to the ferroelectric c axis. At high temperatures in the cubic phase, the band gap decreases at the rate -4.5×10^{-4} eV/°C. EA measurements in the tetragonal phase show that an applied electric field along the c axis shifts the entire Urbach edge rigidly upward in energy by an amount $\Delta\mathcal{E}$, which is proportional to the square of the total polarization P , spontaneous plus field-induced, i.e., $\Delta\mathcal{E} = \beta P^2$. The effect can be described by a temperature-independent band-edge polarization potential β having the value $\beta_{11} = 1.16$ eV m⁴/C². The smaller β_{12} coefficient could not be measured, because of photoconductivity and carrier-trapping effects. An anomalous increase in the band gap with decreasing temperature within 150 °C of the Curie point is attributed to coupling between polarization fluctuations and the band edge. A simple thermodynamic model is shown to describe the temperature dependence of this fluctuation contribution with reasonable accuracy. The results suggest that the correlation volume V_c is at most a weak function of temperature and that V_c does not display critical behavior. This conclusion is consistent with several recent experiments in displacive ferroelectrics. The magnitude of the observed mean square polarization fluctuation contribution to the band-edge position (≈ 15 meV at $T = T_C$) can be understood using the simple fluctuation theory with the value $V_c \approx 4.5 \times 10^4$ Å³ deduced previously from photoelastic constant measurements. It is also suggested that a mean square polarization fluctuation contribution to the band-edge position is present in the tetragonal phase below approximately 100 °C owing to the proximity of the tetragonal-orthorhombic transition. A fluctuation contribution of about 40 meV is indicated at room temperature.

I. INTRODUCTION

Several studies of the optical-absorption edge in BaTiO₃ have been reported. Casella and Keller¹ and Gähwiller² find a broad absorption tail extending to nearly 2.5 eV, while Cox *et al.*³ have attempted

to fit similar absorption data to well-known formulas. Gähwiller² has also reported results of electroabsorption (EA) experiments in the vicinity of the band edge and related the field-induced band-edge shifts to crystal polarization. Recently, DiDomenico and Wemple⁴ have shown that these ab-

sorption and electroabsorption results were actually not related to properties of the pure crystal but were in fact dominated by impurities that appear to be unavoidable in samples grown from a KF flux.⁵ In the purer top-seeded solution-grown (melt-grown) crystals,⁶ the interband absorption edge displays Urbach-rule behavior,^{4,7} i. e., the absorption coefficient increases exponentially with increasing photon energy, and there is consequently no uniquely defined band gap. An Urbach edge is also observed in the perovskite oxides SrTiO_3 ,⁸ KTaO_3 ,^{9,10} and $\text{KTa}_{0.65}\text{Nb}_{0.35}\text{O}_3$,⁴ so that such behavior appears to be an inherent characteristic of this class of materials. In the present paper, we report results of a more complete investigation of the optical-absorption edge in melt-grown BaTiO_3 than given previously. Absorption data are presented in both the tetragonal and cubic phases to a temperature of 450 °C, and EA results are reported as a function of temperature in the tetragonal phase. The experimental observations are discussed with special reference to the influence of crystal polarization on the band-edge position. In particular, we show that polarization fluctuations affect the band edge and that these fluctuations are directly observable in the optical experiments. A brief preliminary account of this work was reported previously.¹¹

II. ABSORPTION MEASUREMENTS

All absorption measurements were made using single-domain crystals prepared and poled as described elsewhere.¹² A sample-in-sample-out procedure was used, and corrections for surface and multiple internal reflections were made using previously published refractive index data^{12,13} and well-known formulas. The experimental apparatus consisted of a Perkin-Elmer double-pass glass prism monochromator in conjunction with a xenon arc lamp, photomultiplier detector, and a 13-Hz lock-in detection system. The sample was contained in an oven capable of heating the crystal to the vicinity of 450 °C. Care was taken to limit the monochromator resolution to less than 5 Å to prevent the spectral width from influencing the observed Urbach-edge slope. Some representative absorption results at selected temperature are shown in Fig. 1. At 23 °C, two Urbach edges are indicated, corresponding to light polarized parallel (α_{\parallel}) and perpendicular (α_{\perp}) to the tetragonal c axis. We find that $\alpha_{\perp} > \alpha_{\parallel}$, and, in agreement with previous measurements,⁴ the two edges are very nearly parallel and are separated by 108 meV. With increasing temperature, both edges shift to lower energy and their slopes decrease. The tetragonal-cubic transition occurred at 132 °C in these melt-grown crystals so that only a single absorption edge is present above this temperature.

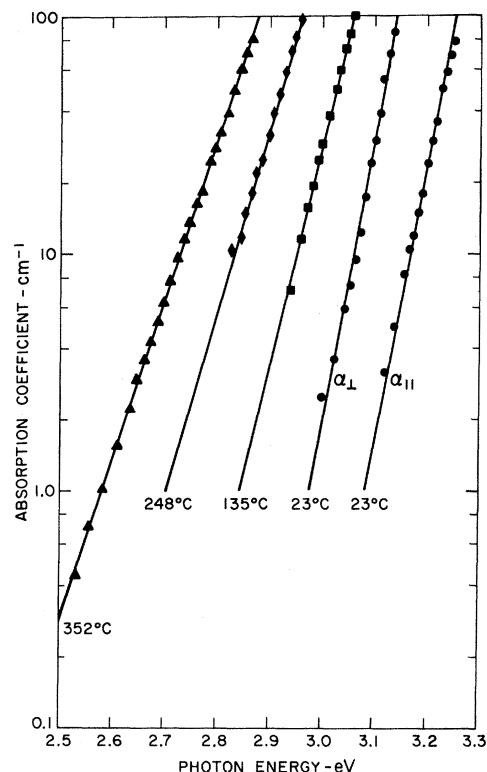


FIG. 1. Representative absorption versus photon energy data near the interband edge in BaTiO_3 . Below the Curie point at 132 °C the two edges correspond to light polarized parallel (α_{\parallel}) and perpendicular (α_{\perp}) to the tetragonal c axis.

It is of interest to compare our 23 °C data with those obtained by Gähwiller² using flux-grown crystals. This comparison is shown in Fig. 2 where we have indicated by the dotted line an extension of the Urbach edge beyond the range of absorption coefficients observed in the present study. This extension is justified by the previously reported⁴ occurrence of Urbach-rule behavior to an absorption coefficient of almost 10^3 cm^{-1} . It is clear from Fig. 2 that the Urbach edge blends into Gähwiller's data for absorption coefficients above $3 \times 10^3 \text{ cm}^{-1}$. The extra impurity-related absorption in the flux-grown samples is plotted as a function of photon energy in Fig. 3. Note that the impurity-band peaks appropriate to the two light polarization directions are separated by very nearly the same energy as the two corresponding Urbach tails (i. e., $\sim 108 \text{ meV}$). This result suggests that the electronic states responsible for the impurity absorption may lie just above the valence-band edge. In order to estimate the number of impurity centers required to account for the absorption bands of Fig. 3, we make use of a relation¹⁴ derived in the context of

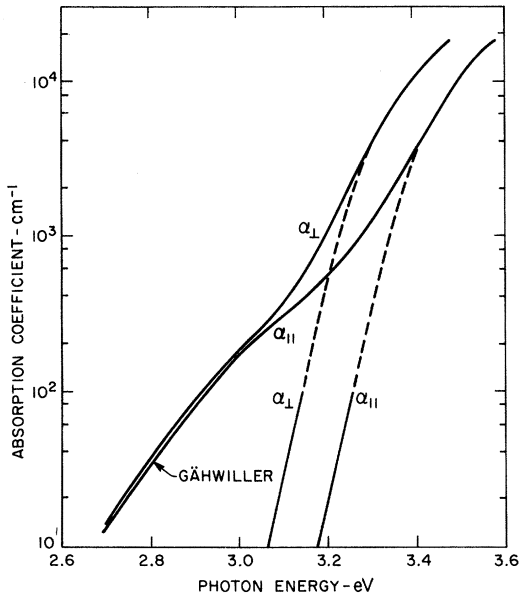


FIG. 2. Comparison of room-temperature absorption-edge data in flux-grown BaTiO_3 (see Ref. 2) and melt-grown crystals. The dotted extension of the curve for melt-grown crystals is blended smoothly into the data of Ref. 2.

F centers and assume that the oscillator strength is ~ 0.5 . The result is a center concentration of $\sim 10^{18} \text{ cm}^{-3}$. The nature of these centers is not

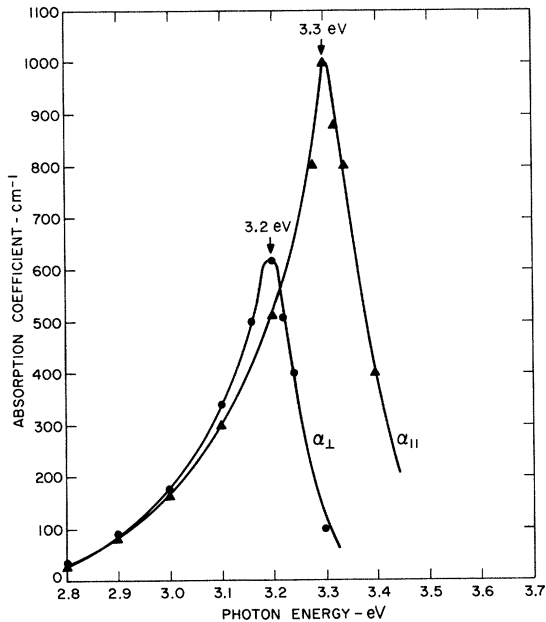


FIG. 3. Impurity-related absorption bands found in flux-grown crystal of BaTiO_3 .

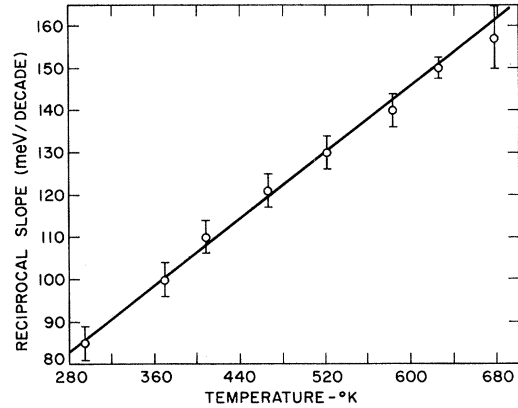


FIG. 4. Temperature dependence of reciprocal Urbach-tail slope in BaTiO_3 . The solid line is given by Eq. (1) of the text.

known at present; however, Arend and Novak¹⁵ have shown that even in their purest (undoped) samples the Fe content was of this order of magnitude while the K and F concentrations were an order of magnitude higher. It is possible, of course, that flux-vacancy complexes may also be involved.

Returning to the absorption characteristics of melt-grown crystals, we turn now to a more detailed examination of the Urbach-edge slope and its temperature dependence. Using data similar to those shown in Fig. 1, we can determine the temperature dependence of the Urbach-tail slope, or to be more precise, the reciprocal slope S in meV/decade. Results are shown in Fig. 4 where a linear relationship between the reciprocal slope and temperature is evident. The solid line is given by the expression

$$S = 2.3k(T + T_0), \quad (1)$$

where $T_0 = (140 \pm 10)^\circ \text{K}$ ($kT_0 = 12 \pm 1 \text{ meV}$), T is the absolute temperature, and k is Boltzmann's constant. The experimentally determined Urbach tail in BaTiO_3 is thus governed by the relation

$$\alpha = \alpha_0 \exp [(h\nu - E_0)/k(T + T_0)]. \quad (2)$$

In Eq. (2), α_0 and E_0 are constants which cannot be separately determined, and $h\nu$ is the photon energy. The form of the Urbach edge given by Eq. (2) is exactly that observed by Frova¹⁰ in the cubic perovskite KTaO_3 . Furthermore, Frova also finds that $T_0 \approx 140^\circ \text{K}$ in this material so that the same effective temperature $T^* = T + T_0$ describes the Urbach edge in both BaTiO_3 and KTaO_3 . In SrTiO_3 , on the other hand, it has been found⁸ that $T_0 \approx 50^\circ \text{K}$.

There is an additional observation connected with the Urbach-edge temperature dependence in BaTiO_3 . We find no significant change in slope on passing

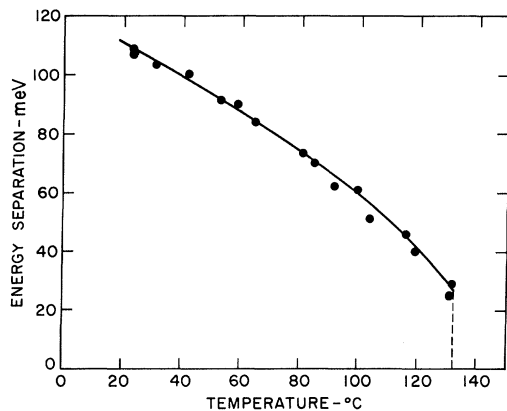


FIG. 5. Temperature dependence of band-edge separation $\Delta\epsilon$ in the tetragonal phase of BaTiO_3 .

through the tetragonal cubic transition at 132°C . This would suggest that the soft transverse optic phonon associated with the ferroelectricity is not an important contributor to the band-edge tail. Other phonons must dominate as discussed in Sec. V.

III. INFLUENCE OF SPONTANEOUS POLARIZATION ON ABSORPTION EDGE

According to Fig. 1, the energy separation $\Delta\epsilon$ between the absorption edges for light polarized parallel and perpendicular to the tetragonal c axis is 108 meV at 23°C . The complete temperature dependence of this separation is plotted in Fig. 5. As expected, the separation decreases with increasing temperature and disappears at the first-order phase transition temperature T_c . At the transition, the parallel and perpendicular edges decrease discontinuously in energy by 36 ± 4 and 11 ± 4 meV, respectively, and coalesce. Because the order parameter which measures the extent of tetragonality in BaTiO_3 is the spontaneous polarization P_s , we expect $\Delta\epsilon$ to depend on even powers of P_s . In Fig. 6 we have plotted $\Delta\epsilon$ versus P_s^2 using P_s -versus-temperature data reported elsewhere.¹² It is clear that $\Delta\epsilon$ increases somewhat more rapidly than P_s^2 . In Sec. V we attribute the observed deviations from an exact quadratic dependence to the influence of polarization fluctuations.

IV. ELECTRIC FIELD DEPENDENCE OF BAND EDGE

Electric-field-induced modulation of the optical transmission in the vicinity of the Urbach edge has been observed using techniques similar to those described by Gähwiller.² A 13-Hz square-wave unipolar voltage was applied along the crystal c axis, and polarized light was propagated parallel to a

crystal a axis. The modulated transmission at 13 Hz was then detected using a calibrated lock-in detection system. Measurements were made as a function of electric field, photon energy, and temperature in the tetragonal phase between 19 and 130°C . The applied voltage was always selected to fall in the region of linearity between the modulation signal and the electric field.

Using a valid approximation⁴ to the usual multiple reflection transmission equation given elsewhere, it can be shown that the fractional change in light transmission $\Delta t/t$ induced by an electric field is given closely by

$$\Delta t/t = -\alpha d(1 - 2R^2 t^2)^{-1} \Delta\alpha/\alpha. \quad (3)$$

Here t is the transmission coefficient, R is the single-surface reflectivity, α is the absorption coefficient, and d is the sample thickness. In our experiments, $t \leq 0.3$ and $R \approx 0.2$, so that the multiple-reflection correction given by $2R^2 t^2$ in Eq. (3) can be entirely neglected. The fractional change in absorption $\Delta\alpha/\alpha$ can be related to changes in the parameters which describe the Urbach tail by differentiating Eq. (2) with the result

$$\begin{aligned} \Delta\alpha/\alpha = & -\Delta E_0/k(T + T_0) + \Delta\alpha_0/\alpha_0 \\ & + (E_0 - h\nu)\Delta T_0/k(T + T_0)^2. \end{aligned} \quad (4)$$

It is unlikely that the applied electric field alters T_0 since, as noted above, this quantity is not significantly affected by the spontaneous polarization. Furthermore, even if the fractional changes in E_0 , α_0 , and T_0 were all of comparable magnitude, the term containing ΔE_0 in Eq. (4) would dominate. To

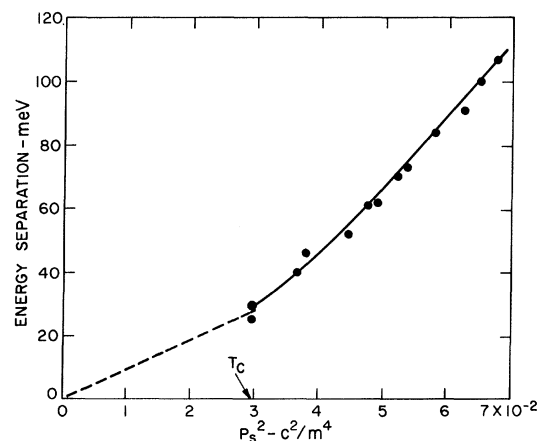


FIG. 6. Dependence of band-edge separation in the tetragonal phase on the square of the spontaneous polarization P_s^2 . The indicated lines serve only to emphasize the observed nonlinear behavior.

show this, we can substitute $E_0 \approx 3.5$ eV, $k(T + T_0) \approx 0.035$ eV, and $E_0 - h\nu \approx 0.2$ eV into Eq. (4) which then becomes

$$\Delta\alpha/\alpha \approx 100\Delta E_0/E_0 + \Delta\alpha_0/\alpha_0 + 2\Delta T_0/T_0. \quad (5)$$

Thus, neglecting the $\Delta\alpha_0$ and ΔT_0 terms, Eqs. (3) and (4) yield

$$\Delta t/t = (\alpha d)\Delta E_0/k(T + T_0). \quad (6)$$

According to Eq. (6), the EA signal should be proportional to the absorption and thus should increase exponentially with photon energy. To verify this expectation, the wavelength dependence of the EA signal was measured at several temperatures between 23 and 130 °C. The results at 71 °C are shown in Fig. 7 for light polarized along the c axis. The exponential dependence is confirmed, and the reciprocal slope is the same as observed for α (i.e., 96 meV/decade). The effect of the electric field is thus simply a *rigid* upward shift of the Urbach tail by ΔE_0 . Frova¹⁰ found that his EA results in KTaO₃ could be described approximately by a rigid upward shift. For temperatures below 40 °C the EA signal appeared to deviate significantly from the exponential behavior predicted by Eq. (6). At high photon energies the expected proportionality between $\Delta t/t$ and α was observed; however, at low energies an excess EA signal was present, which, at room temperature, showed considerable structure as a function of wavelength. Careful examination of this excess signal showed that it did not vary linearly with the electric field; in some cases the signal actually decreased with increasing field. Furthermore, a nonsystematic time dependence was observed with a time constant of the order of 1 min. A very strong temperature dependence was also found with the excess signal decreasing rapidly with increasing temperature and disappearing at approximately 40 °C. These results suggest that photoexcitation of carriers and trapping are playing important roles. For EA measurements, using light polarized perpendicular to the c axis, this defect-related process dominated at all temperatures and photon energies, so that no reliable data could be obtained for this geometry. In the parallel geometry (below 40 °C) only the observations at high photon energy where $\Delta t/t \propto \alpha$ were used in computations of the EA signal.

In Fig. 8 we show the temperature dependence of the EA signal for an applied electric field of 1800 V/cm, an optical path length of 0.975 mm, and an absorption coefficient of 20 cm⁻¹. The observed rapid increase in the EA signal with temperature is a straightforward consequence of the temperature-dependent dielectric behavior of BaTiO₃. To show this we assume, following Frova¹⁰ and Gähwiller,² that the Urbach-edge shift ΔE_0 depends

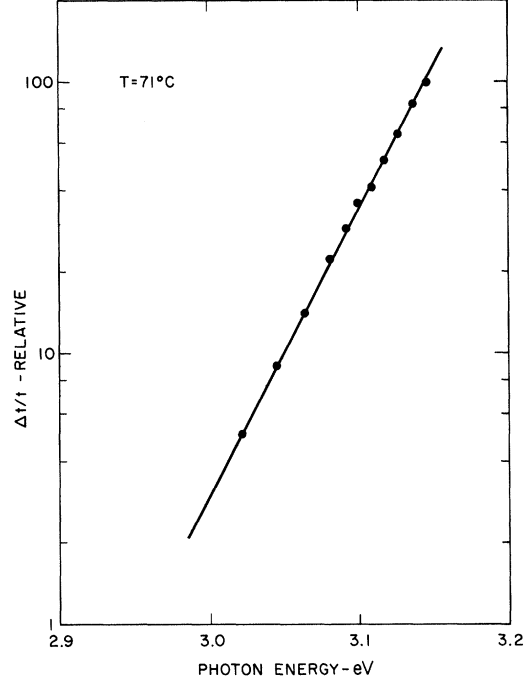


FIG. 7. Dependence of relative electroabsorption signal on photon energy at 71 °C.

only on the crystal polarization and that the effect is fundamentally a biased quadratic effect where

$$\Delta E_0 = 2\beta_{11}P_s\delta P. \quad (7)$$

Here β_{11} is the quadratic band-edge polarization potential, $\delta P = (\kappa_c - 1)\epsilon_0 E$ is the field-induced polarization, κ_c is the c -axis unclamped relative dielectric constant, and ϵ_0 is the free-space permittivity. Substituting Eq. (7) into Eq. (6) yields

$$\Delta t/t = 2(\alpha d)\beta_{11}\epsilon_0(\kappa_c - 1)P_s E/k(T + T_0). \quad (8)$$

Using the EA data shown in Fig. 8 and the values of κ_c and P_s reported elsewhere,¹² we can compute β_{11} from Eq. (8). The result is a temperature-independent polarization potential having the value

$$\beta_{11} = 1.16 \pm 0.05 \text{ eV m}^4/\text{C}^2. \quad (9)$$

As pointed out earlier, photoconduction and carrier-trapping phenomena precluded measurement of β_{12} . In addition, owing to depletion layer formation at the electrodes, it was not possible to reliably measure either β_{11} or β_{12} in the cubic phase, using a dc biasing field to generate a linear effect.¹⁸

V. DISCUSSION

A. Urbach-Edge and Band-Gap Determinations

A detailed theoretical understanding of the Urbach edge is not presently available, although many if

not most ionic crystals display such behavior. The consensus appears to be that phonon-assisted transitions are involved.¹⁷⁻²¹ Kiel¹⁸ and Dunn²⁰ suggest that phonon coupling to the valence electrons is dominant, leading to a substantial tailing above the top of the valence-band edge. None of the existing theories, however, predict the form of the Urbach tail observed in BaTiO₃ and KTaO₃ where $T^* = T + T_0$, and $T_0 = 140^\circ\text{K}$. As suggested by Frova,¹⁰ it is conceivable that the extra band tailing described by the parameter T_0 may be related to impurities; however, there appears to be no reason to expect this effect to be simply describable in terms of an effective temperature T_0 . Furthermore, BaTiO₃ and KTaO₃ are chemically different and are grown at very different temperatures so that it would be surprising if both materials displayed the same impurity-related tailing. It is also puzzling that $T_0 \approx 50^\circ\text{K}$ in SrTiO₃, a material closely related to BaTiO₃. If, indeed, the Urbach tail is produced by phonon coupling to the valence-band p -like electrons, then the following simple physical picture suggests itself. Those phonons which couple strongly to valence electrons cause the valence-band edge to be diffuse, producing the observed Urbach tail. Because, as pointed out earlier, the tail is not significantly influenced by the phase transition in BaTiO₃, it would appear that the soft zone-center transverse optic (TO) phonon is not involved. This view is further supported by the ob-

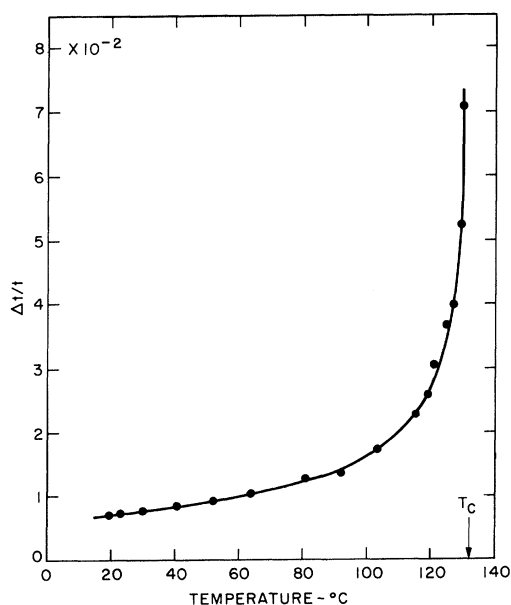


FIG. 8. Temperature dependence of the electroabsorption signal $\Delta t/t$ for an applied field of 1800 V/cm, sample thickness of 0.975 mm, and an absorption coefficient of 20 cm^{-1} .

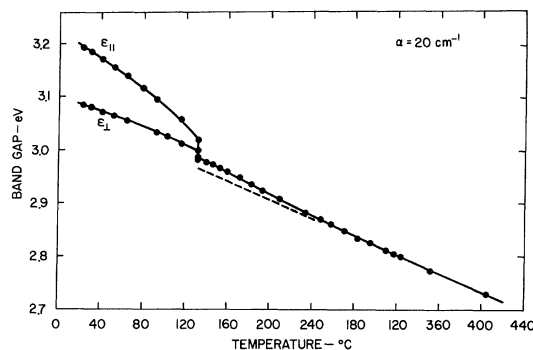


FIG. 9. Temperature dependence of the band gap in BaTiO₃ defined at $\alpha = 20\text{ cm}^{-1}$. The two gaps below 132°C correspond to light polarized parallel ($\alpha_{||}$) and perpendicular (α_{\perp}) to the c axis.

servations that (a) $T_0 = 140^\circ\text{K}$ in KTaO₃ and $T_0 = 50^\circ\text{K}$ in SrTiO₃, while the soft-mode frequencies are nearly the same, and (b) $T_0 = 140^\circ\text{K}$ in BaTiO₃, while the soft-mode frequency is substantially lower than in KTaO₃ and SrTiO₃. Turning to the conduction band, we expect⁴ strong coupling between this band and the crystal polarization associated with the soft mode. Thus, either a dc crystal polarization (see Sec. VB) or polarization fluctuations (see Sec. VC) should couple to the conduction band via the $pd\pi$ interaction and influence the band-edge position. In principle, polarization fluctuations should also influence the band-edge shape, but this does not appear to be a dominant mechanism as suggested by the experimental data.

Although various values of the band gap in BaTiO₃ have been reported in the literature, it is clear, as discussed by Moss,²² that no well-defined band gap exists in a material having an Urbachian edge. A commonly employed stratagem is to arbitrarily define the band gap as occurring at a specified value of absorption coefficient. The experimental results for $\alpha = 20\text{ cm}^{-1}$ are plotted versus temperature in Fig. 9. In the tetragonal phase, two "gaps" are present which decrease substantially with increasing temperature and coalesce above T_C . At high temperatures the gap decreases linearly with temperature at the rate $-8.5 \times 10^{-4}\text{ eV}/^\circ\text{C}$; however, substantial deviations from a linear dependence are observed within 150°C of the Curie temperature. We will subsequently attribute these deviations to the influence of polarization fluctuations, but first it is of importance to establish more realistic band-gap values than those obtained for $\alpha = 20\text{ cm}^{-1}$. To do this we make use of the absorption and EA results reported by Frova¹⁰ for KTaO₃. He finds, using very thin samples, that the absorption increases less rapidly with the photon energy above an absorption coefficient of approximately 10^3 cm^{-1} .

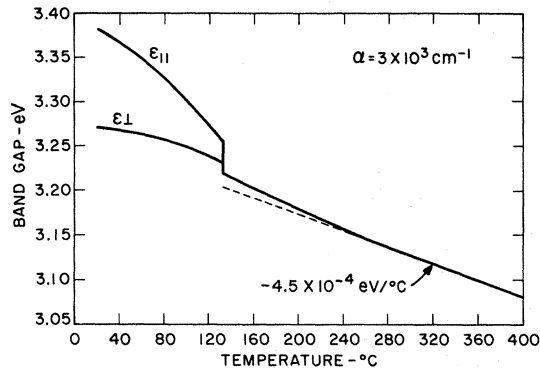


FIG. 10. Temperature dependence of the band gap in BaTiO_3 determined by extrapolation of the Urbach edge to $\alpha = 3 \times 10^3 \text{ cm}^{-1}$ (see text).

than in the Urbach tail. The blending of the Urbach tail in BaTiO_3 with Gähwiller's results (see Fig. 2) show similar behavior. The pertinent results reported by Frova which allow a realistic estimation of the band gap are (i) the shape of the absorption curve is temperature independent in the region of rounding above $\alpha \approx 10^3 \text{ cm}^{-1}$, suggesting that phonons are playing a minor role, and (ii) the EA results show a small peak in the region of rounding. Based on these results we believe that a realistic value for the band gap in BaTiO_3 can be estimated by extrapolating the Urbach tail to an absorption coefficient of $3 \times 10^3 \text{ cm}^{-1}$ using the form of the edge given by Eq. (2). The resulting band-gap energies shown in Fig. 10 are probably not more than 50 meV in error. At room temperature we find band gaps of 3.38 and 3.27 eV, respectively, for light polarized parallel and perpendicular to the ferroelectric c axis. At high temperatures, the gap decreases at the rate $-4.5 \times 10^{-4} \text{ eV/}^\circ\text{C}$, a more or less typical value²² for crystals. It is of interest that the band gaps of BaTiO_3 and SrTiO_3 (Ref. 8) are very nearly the same.

It should be clear from the preceding discussion that no conclusions can be drawn concerning the "direct" or "indirect" nature of the band edge in BaTiO_3 . Lattice phonons are responsible for the band-edge Urbach tail, but the nature of the phonons involved is not known either experimentally or theoretically. The extrapolated band gaps shown in Fig. 10 are probably direct, however, since the absorption coefficient is quite high ($\sim 10^4 \text{ cm}^{-1}$). Furthermore, in the region of rounding above $\sim 10^3 \text{ cm}^{-1}$ Frova¹⁰ finds in KTaO_3 that there is a negligible temperature dependence of the absorption shape.

B. Influence of Crystal Polarization on Band Edge

The influence of the spontaneous polarization in

the tetragonal phase on the band-edge separation $\Delta\mathcal{E}$ is shown in Fig. 6. Nonlinear behavior is evident so that we conclude from these data that $\Delta\mathcal{E}$, contrary to expectations, is not precisely proportional to P_s^2 . In terms of the polarization potentials defined by the expression $\Delta\mathcal{E} = (\beta_{11} - \beta_{12}) P_s^2$, we find that $\beta_{11} - \beta_{12}$ varies between $1.0 \text{ eV m}^4/\text{C}^2$ at $T = T_c$ and $1.6 \text{ eV m}^4/\text{C}^2$ at $T = 23^\circ\text{C}$. The discontinuous band-edge shifts observed at $T = T_c$ can be used to separately determine β_{11} and β_{12} at this temperature with the results $\beta_{11} = 1.2 \pm 0.15$ and $\beta_{12} = 0.3 \pm 0.15 \text{ eV m}^4/\text{C}^2$. These values should be compared with the value $\beta_{11} = 1.16 \pm 0.05 \text{ eV m}^4/\text{C}^2$ determined from EA data in the tetragonal phase. The EA result, however, is independent of temperature, whereas the quantity $\beta_{11} - \beta_{12}$ derived from the influence of spontaneous polarization on the static band-edge positions is significantly temperature dependent, as noted above. It is not possible to separately determine the temperature dependences of β_{11} and β_{12} in the tetragonal phase using Fig. 10 because there is no easily established reference point from which the energy shifts can be measured. Thus, it is not clear how one might extrapolate the high-temperature data to a temperature below T_c to yield the required reference energy.

In Sec. V C we give a qualitative argument for attributing differences in the temperature dependence of $\beta_{11} - \beta_{12}$ based on EA and static dichroism measurements to perturbations produced by mean-square polarization fluctuations. First, however, we turn to a discussion of the magnitude of band-edge polarization potentials observed in BaTiO_3 .

By extending the linear-combination-of-atomic-orbital (LCAO) calculation of Kahn and Leyendecker²³ to include the polarization-induced nuclear motions, Brews²⁴ has estimated the energy shifts to be expected for various interband critical points. He finds that a value $\beta \sim 1 \text{ eV m}^4/\text{C}^2$ is expected and that the principle physical origin of the shift is very likely a modulation of the $pd\pi$ overlap integral by the motion of Ti atoms towards a nearest-neighbor oxygen atom, although changes in the Madelung potential may be a significant factor, as discussed by Gähwiller.² More detailed discussions of the physical origin of polarization potentials in perovskite-type ferroelectrics are given elsewhere.^{4, 25, 26} For our present purposes we can only conclude that the band-edge polarization potentials observed in BaTiO_3 are of the expected order of magnitude. It is of interest to compare the BaTiO_3 results with those obtained in other perovskite oxides. In KTaO_3 , Frova¹⁰ finds that $\beta_{12} \approx 1.9 \text{ eV m}^4/\text{C}^2$, and in $\text{KTa}_{0.65}\text{Nb}_{0.35}\text{O}_3$, DiDomenico and Wemple⁴ report that $\beta_{11} - \beta_{12} \approx 2.2 \text{ eV m}^4/\text{C}^2$. These values are not qualitatively different from those observed in BaTiO_3 , although it would appear, from the limited data

available, that the band-edge polarization potentials in BaTiO_3 tend to be somewhat small. In this connection it is important to recognize that all these polarization potentials apply in the *unclamped* experimental situation so that energy shifts induced by electrostrictive (or piezoelectric) strain are included in the total observed effect.

The polarization potentials associated with other interband critical points may, of course, differ from those reported here for the band edge, although based on the work of Brews,²⁴ they should be of comparable magnitude. An "average" interband polarization potential $\bar{\beta}$ can be defined²⁷ in terms of shifts of the "average" interband oscillator that describes the refractive index and its dispersion. Using unpublished refractive-index¹³ data and an oscillator description of the form²⁸

$$n^2 - 1 = \mathcal{E}_D \mathcal{E}_0 / [\mathcal{E}_0^2 - (h\nu)^2], \quad (10)$$

where \mathcal{E}_D is the dispersion energy, \mathcal{E}_0 is the single-oscillator energy, and $h\nu$ is the photon energy, we find that $\Delta\mathcal{E}_0 = (\bar{\beta}_{11} - \bar{\beta}_{12}) P_s^2$ with $\bar{\beta}_{11} = 6.3 \text{ eV m}^4/\text{C}^2$ and $\bar{\beta}_{12} \approx 0 \text{ eV m}^4/\text{C}^2$. Detailed discussions of polarization potentials in the contexts of electro-optics and nonlinear optics have been given previously for the entire class of oxygen octahedra ferroelectric.²⁷ For this class of materials it is found that $\bar{\beta} \sim 3 \text{ eV m}^4/\text{C}^2$, a value similar to the band-edge polarization potential observed in the present study. The small value of $\bar{\beta}_{12}$ in BaTiO_3 is unusual, however, and appears to place this material in a somewhat special position. Note, however, that the band edge β_{12} is also small (i. e., $\beta_{12} \approx 0.3 \text{ eV m}^4/\text{C}^2$).

C. Influence of Polarization Fluctuations on Band Edge

As discussed in Sec. VB, crystal polarization, whether spontaneous or field induced, shifts the band edge to higher energy in BaTiO_3 . In this section we examine the possible contributions of polarization fluctuations to the band-edge position assuming that the band-edge tail shape is not affected. The existence of such fluctuations is firmly established on both experimental and theoretical grounds. For example, Raman scattering experiments²⁹ have been used to observe directly the spectral density of polarization fluctuations in the tetragonal phase of BaTiO_3 . The inelastic neutron scattering experiments of Yamada *et al.*³⁰ show clearly both the fluctuations and the presence of correlation in the cubic phase with a correlation length along a polarization $\langle 100 \rangle$ axis of approximately 20 \AA at 137°C . Comes *et al.*³¹ have also deduced, using x-ray data, the existence of short-range order in the cubic phase of BaTiO_3 with a correlation length of roughly 35 \AA . These authors have interpreted their data in

terms of an array of unit cell distortions along $\langle 111 \rangle$ axes rather than in terms of polarization fluctuations. Cochran³² has suggested, however, that their results are in fact consistent with a polarization fluctuation model. In their analysis of electron transport properties of perovskite oxide ferroelectrics in their cubic phases Wemple *et al.*²⁶ have deduced that electron scattering in these materials results from conduction-band-edge perturbations induced by quasistatic polarization fluctuations. This polarization potential scattering is analogous to the deformation potential concept commonly employed to describe scattering by acoustic modes of vibration. These authors also propose a simple physical picture of polarization fluctuations consisting of a three-dimensional array of needlelike clusters which are essentially static when compared with electron relaxation times or optical frequencies. The needlelike shape arises from the strong long-range dipolar forces that lead to intercell correlation and ferroelectric behavior along $\langle 100 \rangle$ directions and the much weaker short-range forces normal to a polar axis which are involved in formation of 180° domain walls. Based on the estimated widths of 180° domain walls ($4\text{--}20 \text{ \AA}$) and the correlation length deduced by Yamada *et al.*²⁷ (20 \AA), each fluctuation cluster is estimated to have the approximate volume of $V_c \approx 10^4 \text{ \AA}^3$. Experimental evidence has been presented^{26,33,34} indicating that this correlation volume is weakly temperature dependent in the sense that no critical behavior associated with the nearby phase transition is evident. This same conclusion was recently drawn by Lines³⁵ in connection with effective field theories of ferroelectricity as applied to LiTaO_3 and LiNbO_3 . Lines incorporates strong intercell correlations into his theory and is forced to conclude, using both experimental data and theoretical arguments, that the correlation volume is noncritical and weakly temperature dependent even in the vicinity of the phase transition. No microscopic theory that would account for this behavior is presently available.

Lacking a detailed theory of polarization fluctuations involving anisotropic correlations, we resort to the thermodynamic description that was used previously in the analysis of the electron scattering results.²⁶ That is, we use the fluctuation-dissipation theorem and write the expression³⁶

$$\langle P^2 \rangle = kT\epsilon^*/V_c, \quad (11)$$

where $\langle P^2 \rangle$ is the mean square polarization fluctuation averaged over the volume V_c , ϵ^* is now the *clamped* dielectric constant, and kT is the thermal energy. In a more detailed analysis it would be necessary to know all the Fourier components of

the fluctuation (i.e., its q dependence); the q dependence of the interaction under consideration would then be required, and finally integration over all q vectors would lead to the final result. None of these steps is possible at present, however, so that we essentially use Eq. (11) to define a correlation volume V_c . It should be clear that V_c is an experimental quantity and is not necessarily the same as the cube of the correlation length l_c observed by Yamada and Shirane.³⁰ Thus, these authors find that l_c is critical, whereas we find that V_c is almost temperature independent and noncritical. The difference, of course, is due to the fact that ϵ^x is explicitly introduced into Eq. (11).

Returning now to the temperature dependence of the band gap of BaTiO₃ shown in Fig. 10, we consider the small deviations from linearity, $\Delta\epsilon_f$, observed within 150 °C of the transition temperature in the cubic phase. Subtracting the linear extrapolation given by the dotted line from the band gap versus temperature curve, the results shown by the dotted line in Fig. 12 are obtained. The solid line in Fig. 11 is a plot of Eq. (11) normalized to the value 15 at $T = T_c$ for comparison with the $\Delta\epsilon_f$ results. We have assumed that $V_c = \text{const}$ and the ϵ^x data were obtained from Ref. 12. The two curves are in qualitative agreement, considering the experimental errors in the band gap, the uncertainties inherent in the linear extrapolation from the high-temperature data, and the possibility of a weakly temperature-dependent correlation volume. The anomalous increase in the band gap above the Curie temperature observed in BaTiO₃ thus appears to be attributable to coupling between polarization fluctuations and the band edge via the polarization potential interaction. The magnitude of the polarization fluctuation-induced energy-band shift $\Delta\epsilon_f$ is also reasonable. To show this we substitute¹² $\epsilon^x = 8000\epsilon_0$ and $T = T_c = 405^\circ\text{K}$ into Eq. (11). The

result is

$$\Delta\epsilon_f = \langle\beta^c\rangle \langle P^2 \rangle = 4 \times 10^5 \langle\beta^c\rangle / V_c \text{ meV}, \quad (12)$$

where $\langle\beta^c\rangle$ is a spatially averaged *clamped* (zero strain) polarization potential seen by a ray traversing the crystal, and V_c is the correlation volume in Å³. Because the contribution of electrostriction to the observed zero-stress band-edge polarization potential is not known, the value of $\langle\beta^c\rangle$ can only be estimated to be of the order of 1 eV m⁴/C². Taking³³ $V_c \approx 5 \times 10^4 \text{ Å}^3$, we then obtain at $T = T_c$ the value $\Delta\epsilon_f \approx 20 \text{ meV}$ in agreement with the observed value of $\approx 15 \text{ meV}$. The magnitude agreement should not be taken too seriously since $\langle\beta^c\rangle$ is not known precisely; however, the results show that polarization fluctuations can account for both the magnitude and temperature dependence of the anomalous band-edge shift shown in Fig. 10 using "reasonable" values for the physical parameters. We point out also that the size of the *average* shift implies dynamic band-edge fluctuations of at least 30 meV so that the electron scattering mechanism suggested in Ref. 26 is given strong support.

As pointed out in Sec. III, the polarization potential $\beta_{11} - \beta_{12}$ deduced from absorption measurements in the tetragonal phase is significantly temperature dependent whereas the EA results give a temperature-independent value of β_{11} . We now suggest that this apparent discrepancy may result from polarization fluctuations associated with the tetragonal-orthorhombic phase transition near 5 °C. A fluctuation-induced upward shift at room temperature of approximately 40 meV is required to account for the entire temperature dependence, and as noted above, a shift of this magnitude is not unreasonable. Unfortunately, a detailed theory of fluctuations in an anisotropic dielectric is not available, so the agreement cannot be made more quantitative at the present time. In terms of our fluctuation model, the EA results are understandable if the applied field has a negligible influence on the fluctuation contribution to the band-edge position. To indicate the implications of this statement, we write the following expression for the total band-edge shift due to both the spontaneous polarization P_s and polarization fluctuations:

$$\Delta\epsilon = \beta P_s^2 + \langle\beta^c\rangle k T \epsilon^x / V_c, \quad (13)$$

where we anticipate that the second term is approximately 40 meV at room temperature. The incremental shift in $\Delta\epsilon$ can be obtained by differentiating Eq. (13) with respect to the applied field-induced polarization δP . The result is

$$\delta\Delta\epsilon/\delta P \approx 2\beta P_s + 0.046 \ln \epsilon^x / \delta P. \quad (14)$$

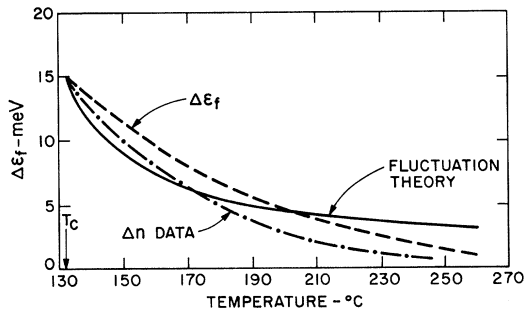


FIG. 11. Polarization fluctuation contribution $\Delta\epsilon_f$ to the band-edge position in the cubic phase (---); normalized prediction of fluctuation model given by Eq. (11) (—); and normalized negative contribution Δn of polarization fluctuations to refractive index (-.-).

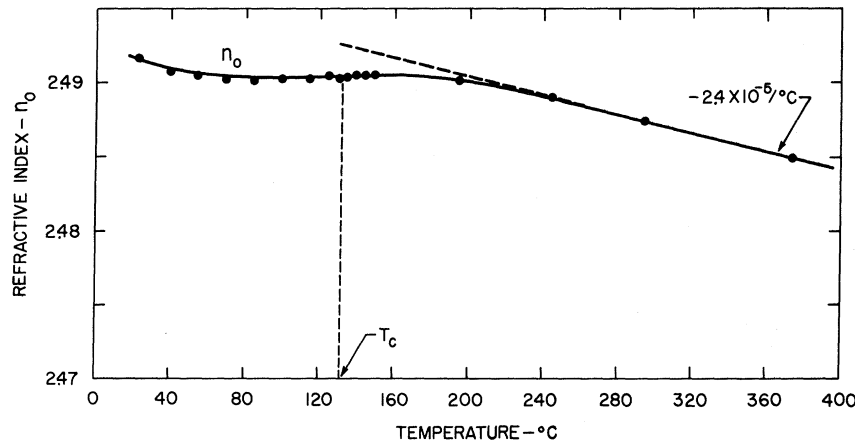


FIG. 12. Temperature dependence of a -axis refractive index in melt-grown crystals of BaTiO_3 for $\lambda = 5145 \text{ \AA}$. The fluctuation contribution is given by the difference between the dashed and solid lines.

The second term in Eq. (14) is the fluctuation contribution to the EA signal. This term may indeed be small compared with the first term which is approximately 0.5, so that a temperature-independent EA value of β may not be surprising. There are, however, no reliable theoretical or experimental values of $\delta \ln \epsilon^* / \delta P$ on which to base a quantitative argument.

D. Influence of Polarization Fluctuations on Refractive Index

If, as suggested above, polarization fluctuations above the Curie temperature raise the band edge via the polarization potential interaction, then a corresponding anomalous *decrease* should be observed in the refractive-index temperature dependence. Hofmann³⁷ has in fact observed just such an effect in flux-grown crystals and invoked polarization fluctuations to account for the observation. Recently, similar data¹³ have been obtained using prisms of melt-grown BaTiO_3 . Results are shown in Fig. 12. The linear decrease in refractive index at high temperatures is of the same magnitude as reported by Hofmann. Within 150°C of the Curie temperature, the refractive index falls below the linear extrapolation and is essentially flat in the immediate vicinity of T_c . It is of interest to note that the a -axis refractive index exhibits no change at the transition (i. e., $\bar{\beta}_{12} = 0$). In Fig. 11 the difference, Δn , between the dashed and solid lines shown in Fig. 12 is plotted as a function of temperature for comparison with the band-edge shift results and the fluctuation theory. For purposes of comparison the curve is normalized so that $\Delta n = 15$ at $T = T_c$. The agreement is within the rather large experimental uncertainties so that both the upward shift in the band edge and the decrease in the refractive index above the Curie temperature appear to be related to the coupling of polarization

fluctuations to the energy bands. The magnitude of the anomalous refractive-index decrease ($\approx 2.5 \times 10^{-3}$ at $T = T_c$) can be qualitatively understood by examining the corresponding upward shift in the single-oscillator energy \mathcal{E}_0 [see Eq. (10)] that describes the refractive-index dispersion. We find that $\Delta \mathcal{E}_0 \approx 20\text{--}30 \text{ meV}$ compared with an upward band-edge shift $\Delta \mathcal{E}_f \approx 15 \text{ meV}$. The two shifts are not expected to be equal since the "average" *inter-band* polarization potential is generally higher, as discussed earlier, than the band-edge value. We conclude that the observed upward shifts $\Delta \mathcal{E}_0$ and $\Delta \mathcal{E}_f$ are qualitatively consistent with one another, but a more detailed comparison cannot be made at the present time.

If there is a contribution to the refractive index due to the influence of polarization fluctuations described by Eq. (11), then application of crystal strain can alter the refractive index through modification of the dielectric constant and thus the amplitude of polarization fluctuations. This fluctuation contribution to the elasto-optic coefficients has been computed recently³³ and shown to contribute a measurable temperature-dependent term. Cohen *et al.*³³ have made a detailed analysis of elasto-optic data in BaTiO_3 above T_c and report quantitative agreement with the fluctuation theory using a value $V_c \approx 4.5 \times 10^4 \text{ \AA}^3$. Furthermore, the temperature dependence of the elasto-optic coefficients reveals that V_c is essentially temperature independent and noncritical, as suggested by both the electron scattering²⁶ and band-edge shift results. Thus, all four experiments, viz., electron scattering, band-edge shift, refractive-index temperature dependence, and photoelastic coefficient temperature dependence support the view that polarization fluctuations are large over an extended temperature range ($\approx 150^\circ\text{C}$) above $T = T_c$, and that the correlation volume V_c is noncritical and has a value of $10^4\text{--}10^5 \text{ \AA}^3$. The

physical meaning of this volume as well as its relationship to the neutron and x-ray scattering results remains an open question.

ACKNOWLEDGMENTS

It is a pleasure to acknowledge the encouragement and advice of Professor H. Gränicher and the staff of the Laboratorium für Festkörperphysik. In particular, the author is indebted to E. Wiesen-

danger and R. Kind for their technical assistance. Thanks are also due M. DiDomenico, Jr., and A. Frova for many suggestions and for reading the manuscript, A. Linz for the excellent crystals of BaTiO₃, and S. Singh for refractive-index data prior to publication. Finally, the author expresses his appreciation to the Zentenarfonds der ETH Zürich for providing financial support during his stay in Zürich.

[†]Experimental work reported here was performed while on leave at the Laboratorium für Festkörperphysik ETH, Zürich, Switzerland.

¹R. C. Casella and S. P. Keller, Phys. Rev. **116**, 1469 (1959).

²Ch. Gähwiler, Phys. Kondensierten Materie **6**, 269 (1967); Solid State Commun. **5**, 65 (1967).

³G. A. Cox, G. G. Roberts, and R. H. Tredgold, Brit. J. Appl. Phys. **17**, 743 (1966).

⁴M. DiDomenico, Jr., and S. H. Wemple, Phys. Rev. **166**, 565 (1968).

⁵J. P. Remeika, J. Am. Chem. Soc. **76**, 940 (1954).

⁶A. Linz, V. Belruss, and C. S. Naiman, J. Electrochem. Soc. **112**, 60C (1965).

⁷F. Urbach, Phys. Rev. **92**, 1324 (1953).

⁸M. I. Cohen and R. F. Blunt, Phys. Rev. **168**, 929 (1968); M. Capizzi and A. Frova (unpublished).

⁹S. H. Wemple, Phys. Rev. **137**, A1575 (1965).

¹⁰A. Frova, Nuovo Cimento **55B**, 1 (1968).

¹¹R. Hofmann, S. H. Wemple, and H. Gränicher, Proceedings of the Second International Meeting on Ferroelectricity, Kyoto, Japan, 1969 (unpublished); J. Phys. Soc. Japan Suppl. (to be published).

¹²S. H. Wemple, M. DiDomenico, Jr., and I. Camlibel, J. Phys. Chem. Solids **29**, 1797 (1968); I. Camlibel, M. DiDomenico, Jr., and S. H. Wemple, *ibid.* **31**, 1417 (1970). The second paper contains the accurate dielectric data that were used in the present study.

¹³S. Singh, S. H. Wemple, M. DiDomenico, Jr., J. R. Potopowicz, and I. Camlibel (unpublished).

¹⁴D. L. Dexter, Phys. Rev. **101**, 48 (1956).

¹⁵H. Arend and J. Novak, Kristall. Technik **1**, 93 (1966).

¹⁶Harmonic detection without recourse to a dc biasing field is, of course, possible in the cubic phase, but this was not done.

¹⁷D. Dunn, Phys. Rev. **166**, 822 (1968).

¹⁷H. Mahr, Phys. Rev. **125**, 1510 (1962); **132**, 1880 (1963).

¹⁸T. H. Keil, Phys. Rev. **144**, 582 (1966).

¹⁹G. D. Mahan, Phys. Rev. **145**, 602 (1966).

²⁰D. Dunn, Phys. Rev. **166**, 822 (1968).

²¹A. S. Davydov, Phys. Status Solidi **27**, 51 (1968).

²²T. S. Moss, *Optical Properties of Semi-Conductors* (Butterworths, London, 1961).

²³A. H. Kahn and A. J. Leyendecker, Phys. Rev. **135**, A1321 (1964).

²⁴J. R. Brews, Phys. Rev. Letters **18**, 662 (1967).

²⁵J. D. Zook and T. N. Casselman, Phys. Rev. Letters **17**, 960 (1966).

²⁶S. H. Wemple, M. DiDomenico, Jr., and A. Jayaraman, Phys. Rev. **180**, 547 (1969).

²⁷M. DiDomenico, Jr., and S. H. Wemple, J. Appl. Phys. **40**, 720 (1969); S. H. Wemple and M. DiDomenico, Jr., *ibid.* **40**, 735 (1969).

²⁸S. H. Wemple and M. DiDomenico, Jr., Phys. Rev. Letters **23**, 1156 (1969).

²⁹M. DiDomenico, Jr., S. H. Wemple, S. P. S. Porto, and R. Bauman, Phys. Rev. **174**, 522 (1968).

³⁰Y. Yamada and G. Shirane, Phys. Rev. **177**, 848 (1969).

³¹R. Comes, M. Lambert, and A. Guinier, Solid State Commun. **6**, 715 (1968); **7**, 305 (1969).

³²W. Cochran, Phys. Status Solidi **30**, K157 (1968).

³³M. G. Cohen, M. DiDomenico, Jr., and S. H. Wemple, Phys. Rev. B **1**, 4334 (1970).

³⁴S. H. Wemple and M. DiDomenico, Jr., Phys. Rev. B **1**, 193 (1970).

³⁵M. E. Lines, Phys. Rev. B **2**, 690 (1970); **2**, 698 (1970).

³⁶See, for example, *Fluctuation Phenomena in Solids*, edited by R. E. Burgess (Academic, New York, 1965).

³⁷R. Hofmann, Ph.D. thesis, Eidgenössische Technische Hochschule, Zürich, Switzerland, 1968 (unpublished).